REASSESSMENT OF FIFTY YEARS OF SEISMICITY IN SIMAV-GEDIZ GRABENS (WESTERN TURKEY), BASED ON CALIBRATED EARTHQUAKE RELOCATIONS

Ezgi KARASOZEN
Department of Geophysics, Colorado School of Mines, Golden, CO, United States.
ekarasoz@mines.edu

Edwin NISSEN
Department of Geophysics, Colorado School of Mines, Golden, CO, United States.
enissen@mines.edu

Eric BERGMAN
Global Seismological Services, Golden, CO, United States.
bergman@seismo.com

Keywords: Seismicity and Tectonics, Earthquake Relocation, Interferometry, Normal Faults

ABSTRACT

Western Turkey is one of the most seismically active and rapidly deforming continental regions with a long history of large normal faulting earthquakes. However, the locations and slip rates of the responsible faults are poorly constrained. Here, we reassess a series of large earthquakes in the Simav-Gediz region, an area exhibiting a strong E-W gradient in N-S extension rates, from low rates bordering the Anatolian Plateau to much higher rates in the west. We start by investigating a recent Mw ~ 5.9 earthquake at Simav (19 May 2011) using Synthetic Aperture Radar interferometry (InSAR), teleseismic body-waveform modeling and field observations. This event provided the impetus to reassess older instrumental events in the region using a calibrated earthquake relocation method based on the hypocentroidal decomposition (HD) technique. These improved locations in turn provide an opportunity to reassess the regional tectonics. One interesting aspect of these earthquakes is that the largest (the Mw 7.2 Gediz earthquake, March 1970) occurred in an area of slow extension and indistinct surface faulting, while the well-defined and more rapidly extending Simav graben is associated with several smaller Mw 5.0 – 5.9 events. Since the faulting is so poorly characterized, the risks posed to nearby cities are also little understood. Whilst our geographical focus is on western Turkey, the strategy we employ in this study could potentially be exploited in other areas in which poorly understood, early instrumental events warrant reinvestigation.

1. INTRODUCTION

Western Turkey is a rapidly-extending continental region with a long history of destructive normal faulting earthquakes including several large instrumental events. It is bound by the right-lateral North Anatolian fault to the north, the Anatolian plateau to the east, the Cyprus Arc and Hellenic Trench to the south, and the Aegean Sea to the west. GPS velocities show maximum N-S extension rates of ~30 mm/yr along the Aegean coastline at a longitude of ~27°E, diminishing to zero east of ~32° E (Aktug et al., 2009).

Extension is expressed in the regional topography by a series of approximately E-W-trending graben and half-graben and in crustal thicknesses, which are thinner in western Turkey (25–35 km) than in central and eastern Anatolia (35–45 km and 45–55 km, respectively) (Vanacore et al., 2013). In general, normal faults closer to the Aegean have greater relief and longer segment lengths, and are presumably older, than those bordering the rigid Anatolian plateau in the East. This gradient in deformation could provide insights on the development of normal faulting through time. However, a simple space-for-time substitution is complicated by the potential involvement of structures inherited from earlier phases of shortening and extension during the Cenozoic.

In this study, we investigate a series of large earthquakes in the Simav-Gediz region (Fig.1) which illustrate many of the gaps in our understanding of fault kinematics in western Turkey. We start by characterizing the recent Mw 5.9 Simav earthquake of 19 May 2011 and its aftershock sequence using an assortment of modern data which include Synthetic Aperture Radar interferometry (InSAR) and dense regional seismic recordings. This event is then used as a catalyst to reassess older instrumental events in the region using a cutting-edge calibrated earthquake relocation method. Of particular interest to us are the Mw 7.2 Gediz earthquake of 28 March 1970, which remains the largest instrumentally-recorded normal faulting event in western Turkey, and the Mw 5.9 Demirci earthquakes of 23 and 25 March 1969. The faults responsible for these older events remain uncertain due in part to large errors in their epicenters, and there have been controversial suggestions that these events involved slip on basal, low-angle detachment faults (Eyidogan and Jackson, 1985; Braunmiller and Nabelek , 1996; Seyitoglu, 1997; Gurboga, 2013).

2. SEISMICITY

Instrumentally-recorded seismicity in our study area can be spatially and temporally divided into three subsets (Fig. 1): (1) the Simav sequence which includes the 2011 Mw 5.9 event and its aftershocks in the eastern Simav depression (2) the Gediz sequence which includes the Mw 7.2 earthquake near Gediz, in the eastern part of our study area, (3) the Demirci sequence starting in 1969 in the western Simav depression, with magnitudes as high as Mw 5.9.

2.1. 2011 SIMAV EARTHQUAKE AND ITS AFTERSHOCKS

The 19 May 2011 Simav earthquake occurred at the eastern end of Simav graben (Fig.1). Although this was a moderate magnitude (Mw = 5.9) earthquake, 2 people were killed, about 100 people were injured and around 2,000 households were heavily damaged or collapsed (Zulfikar et al., 2011). This area experienced a smaller earthquake (Mw = 4.9) in approximately the same location at February, 17 2009. Both earthquakes have similar normal mechanisms consistent with NW-SE trending faulting (Gorgun, 2014).

We used long-period body waveforms to determine the source parameters of the 2011 Simav earthquake. We used seismograms recorded by Global Seismic Network in the distance range of 30^o to 90^o so as to avoid complications form Earth's crust and outer core. Then, we inverted the P and SH waveform data to find the best-fit strike, dip, rake, scalar moment, centroid depth and source time function for a point source. We modeled P,pP and sP phases on vertical components and S, sS phases on transverse components and assumed an elastic half space with Vp = $6km^{-1}$ and Vs=3.5 km^{-1}. Arrival times were checked against broadband records before the inversion, to prevent any potential biases that could arise from epicentral mislocation. The bodywave solution for the Simav earthquake (Fig. 2) has a clear normal faulting mechanism with a strike of 289°, dip of 54° and a centroid depth of 8 km for the NNE-dipping nodal plane, in good agreement with other published solutions.

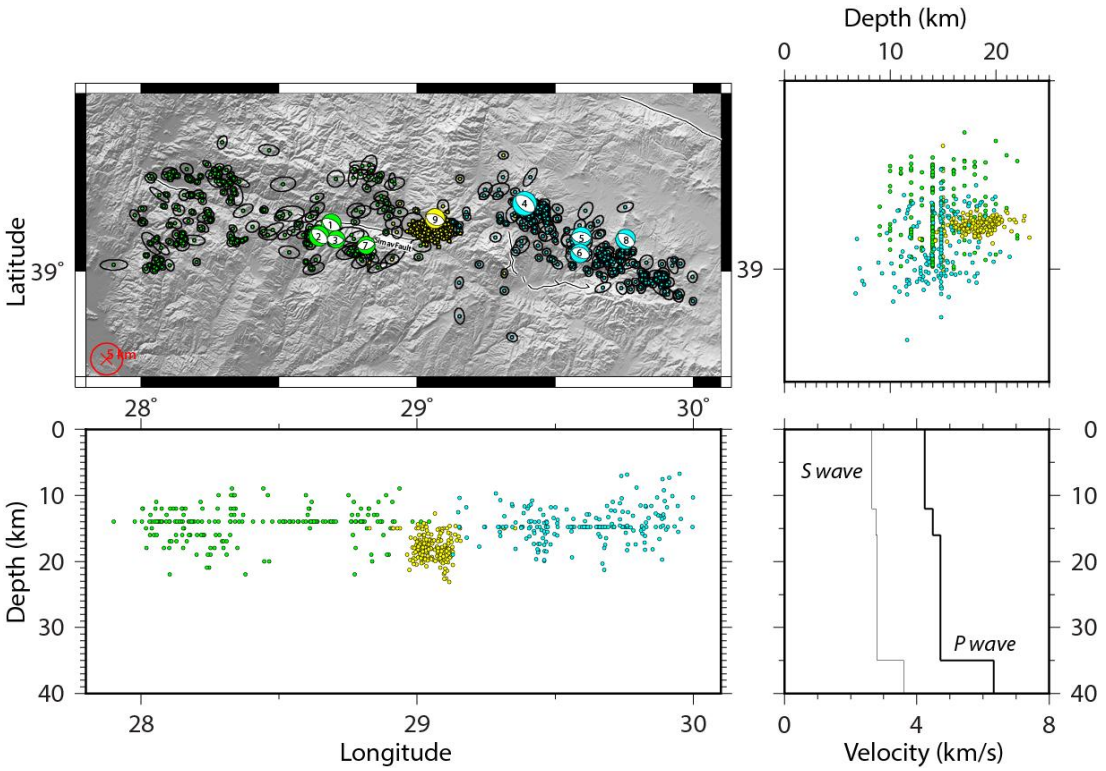

Figure 1. Earthquake locations after relocation for Demirci, Simav and Gediz clusters, indicated by green, yellow and magenta respectively. The velocity model obtained during the relocation process is shown in the lower left panel. See Table 1 for the focal mechanism information.

Ground deformation measured with Interferometric Synthetic Aperture Radar (InSAR) provides additional constraints on the source mechanism of the earthquake and allows us to determine the location of the ruptured fault plane. The coseismic interferogram of Simav earthquake is constructed from ENVISAT descending track scenes acquired in 6 May 2011 and 15 June 2011with a 41◦ center scene incidence angle. The small, but clear earthquake signal comprises an elliptical, WSW- ENE trending fringe pattern containing peak displacements of three radar half-wavelengths (~8.5 cm) away from the satellite(Fig. 3a). We used elastic dislocation modeling (Okada, 1985) to obtain fault plane parameters that are independent from seismology. We initially assumed uniform slip on rectangular fault planes, and tested both north and south dipping faults separately. There is no clear discontinuity in the interferograms which is consistent with the lack of primary surface rupturing observed in the field, and our modeling suggested that the fault plane is buried to a depth of ~6 km. The surface projection of the faulting can be either at the northern or southern edge of the elliptical fringe pattern. We find that the fault strike is poorly resolved by the InSAR modeling and so we fixed it to match the strike of the nodal planes of the body-waveform model. The fault models shown in Figure 3 are obtained using a strike of 289◦ (Model A) and 117◦ (Model B), with dips of 38° and 36° respectively. The depth of the fault plane center is 8-9 km, in good agreement with the body-waveform centroid depth. However, only the N-dipping fault (Model A) is consistent with clear faulting expressed in the topography- the eastern end of the Simav fault (Fig.3b). We suspect that it was a buried patch of this fault that slipped during the 19 May 2011 earthquake.

Table 1. Focal mechanism parameters of the earthquakes shown in Figure 1. Data are taken from body-waveform modelling or the Global Centroid Moment Tensor (GCMT) or National Earthquake Information Center (NEIC) catalogs.

No.	Date	Time	Long.	Lat.	Mw	Strike	Dip	Rake	Cluster
1	1969.03.23	21:08:43	28.49	39.124	5.9	296	54	-92	Demirci
2	1969.03.25	13:21:32	28.467	39.199	5.6	307	44	-96	Demirci
3	1969.04.30	20:20:32	28.553	39.14	5.1	78	39	-114	Demirci
4	1970.03.28	21:02:23	29.545	39.175	7.2	304	41	-87	Gediz
5	1970.04.16	10:42:18	29.914	39.003	5.6	283	38	-102	Gediz
6	1970.04.19	13:29:36	29.772	38.992	5.9	278	50	-87	Gediz
7	1970.04.23	9:01:24	28.676	39.13	5.2	77	50	-96	Demirci
8	1971.05.25	5:43:27	29.73	39.029	5.9	297	51	-102	Gediz
9	2011.05.19	20:15:23	29.124	39.115	5.9	285	60	-90	Simav

2.2. 28 MARCH 1970 GEDIZ EARTHQUAKE AND ITS AFTERSHOCKS

The 28 March 1970 Gediz earthquake is one of the most destructive earthquakes in western Turkey's history. According to Ambraseys and Tchalenko (1972) and Tasdemiroglu (1971), 1,088 people were killed and about 20,000 buildings were damaged. It is associated with an unusually complex surface rupture and source mechanism for an earthquake of this magnitude. Faulting associated with the main shock trends both NNW-SSE and E-W (Ambraseys andTchalenko, 1972), forming an overall L-shape, and with displacements of up to2.2 m.

According to an early modeling by Eyidogan and Jackson (1985) , this earthquake has initial slip on steep, NNW-SSE Asikpasa-Muhipler fault segment, then triggered the second subevent on the E-W trending Erdogmus-Hamamlar fault and later moment release on a low-angle NE-dipping fault. But, reanalysis by Braunmiller and Nabelek (1996) supported a simpler source mechanism which involves a single, steep, planar fault.

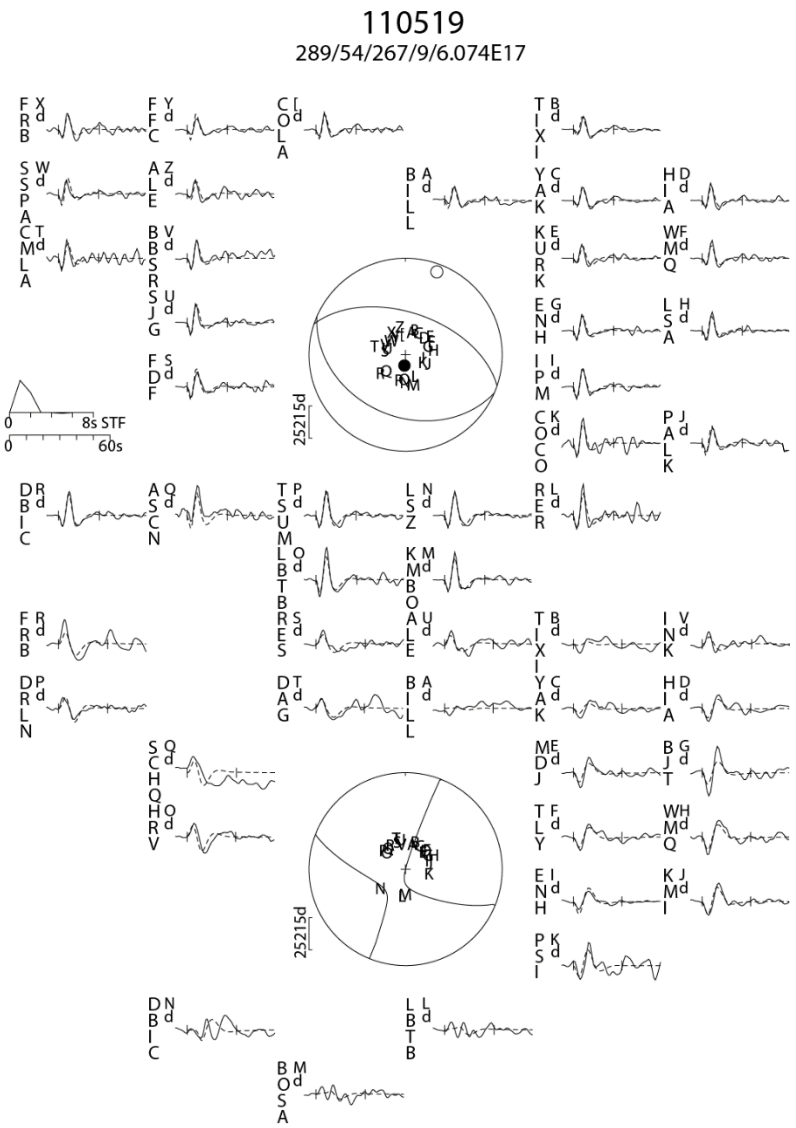

Figure 2. Minimum misfit solution for the May 19, 2011 Simav earthquake calculated by inverting long period P (upper panel) and SH (lower panel) bodywaves. Numbers below the event date show the strike, dip and rake of the NNE-dipping nodal plane; the centroid depth in km; and the moment in Nm.

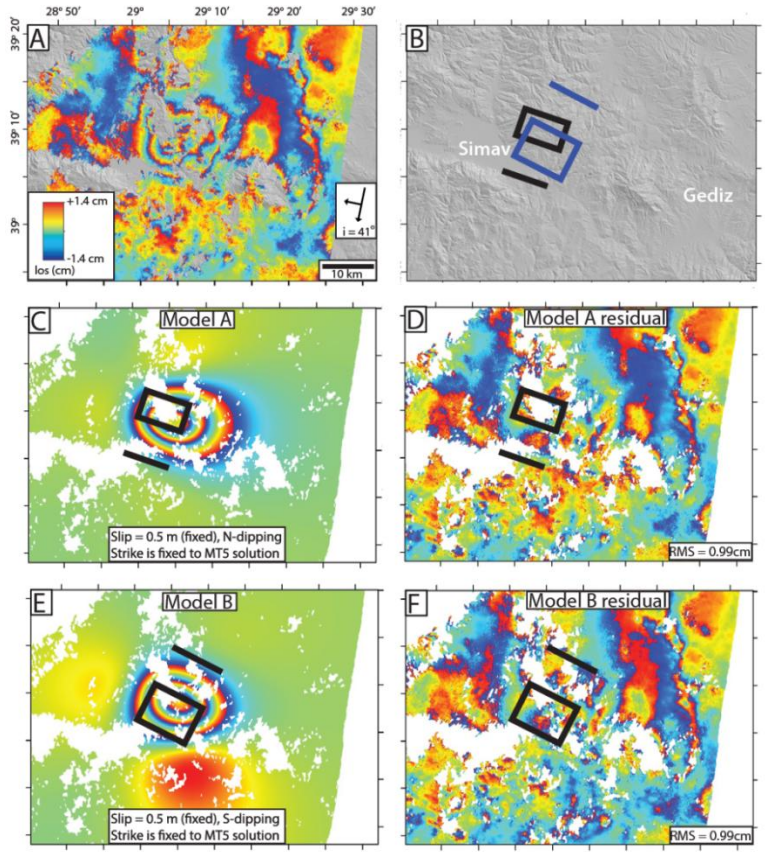

Figure 3. (a) Descendingtrack interferogram spanning the 19 May 2011 earthquake (Mw = 5.9). (b) Conjugate model faults overlain on shaded topography. The boxes show the rectangular model faults in plan view and the lines show their up-dip surface projections. (c) Model and (d) residual (observed minus model) interferogram for a NNE-dipping model fault. (e) Model and (f) residual interferogram for the SSW-dipping case.

2.3. 23 MARCH 1969 DEMIRCI EARTHQUAKE AND ITS AFTERSHOCKS

The Demirci sequence started with a Mw 5.9 earthquake on 23 March 1969, which damaged 1700 buildings without any fatalities (Ambraseys and Tchalenko, 1972). Four aftershocks with magnitude 5 or greater were recorded (Table 1). Their mechanisms indicate E-W faulting in the western part of Simav graben (Eyidogan and Jackson, 1985) with moderately-dipping nodal planes (30^o – 60^o), but there was no surface faulting that could resolve the nodal plane ambiguity. Eyidogan and Jackson (1985) suggested that the mainshock and largest aftershocks ruptured the southerly-dipping fault along the western margin of the Simav graben, which is where the earthquake damage was most prominent. However, Seyitoglu (1997) stated that both the mainshock and April 25, 1969 aftershock are probably associated with the north dipping Simav fault based on an assumed epicenter down-dip of this fault to the north of the Simav graben, and because of the fresh fault surfaces that can be observed on the southern side of the graben.

3. CALIBRATED EARTHQUAKE RELOCATIONS

It is still unclear that which faulting was responsible for the events discussed above, which seeks for earthquake locations that have well-characterized uncertainties and minimal location bias. Therefore, we conducted detailed analyses of the three clusters of earthquakes with the *Mloc* multiple event relocation technique (Bergman and Solomon, 1990; Walker et al., 2011), which is based on the hypocentroidal decomposition (HD) method of Jordan and Sverdrup (1981). This method determines the calibrated locations of all events that meet or exceed a certain level ("GT5") of accuracy, in which the term "calibrated" defines the minimization of location bias that comes from the structure of the Earth. GTX stands for ground truth epicenter location accuracy of X kilometers (Bondar et al., 2004). Furthermore, this location technique calculates confidence ellipses at 90 per cent level which include both the uncertainty of relative location and the uncertainty of the calibration process. The problem of the unknown velocity model of the Earth can be

used as an advantage in multiple-event relocation methods. HD makes use of this by assuming that ray paths from a close spatial cluster of events will largely sample the same portion of the unmodelled Earth and the difference in the traveltimes will reflect the events' relative location. This minimizes the location errors since the method uses traveltime differences rather than absolute traveltimes.

The algorithm is unique in the way that it separates the location problem into two independent inverse problems: (1) it solves for the absolute location of the 'hypocentroid' or geometrical center of the cluster; which is defined as the geometric mean of all of the events in the cluster; then (2) it solves for the relative location of each event in the cluster, the 'cluster vectors', with respect to the hypocentroid.

Location of cluster vectors is more bias free than location of the hypocentroid since it uses the traveltime differences which minimizes the error from the unmodelled Earth. Thus, all available arrival time data (at any epicentral distance) can be used for the location of cluster vectors. The more problematic stage is adding the cluster vectors to the hypocentroid in order to obtain absolute locations. In order to minimize the errors in hypocentroid location, only direct arrival phases (Pg and Sg) at short epicentral distances are used. They are selected up to the nearest distance so that there are still enough readings with a good azimuthal coverage. This two-step inversion usually converges after 2-4 iterations and after each run data set is 'cleaned' according to the empirical reading errors. Analysis of the data sets provides the spread of residuals for each phase since it consists of phase readings from multiple sources in a restricted region.

The success of this relocation technique usually depends on the availability of near- source data, and western Turkey is excellent in this regard as it has dense local station coverage. This allows us to use the direct calibration method, in which we analyze a subset of well-recorded events in the cluster using arrival times at the closest stations. In this study, all relocations are based on 1-D Earth models, and we used the same velocity model for each cluster (Fig. 1). Velocity model determination is done manually by fitting the observed travel time data to the standard theoretical traveltimes (ak135). For crustal phases (Pg, Sg) P and S velocities are adjusted according to the available arrival data in the source region. The upper mantle velocities, together with the thickness of the crust are determined by adjusting the Pn and Sn arrivals. In our velocity model two-layered crust is preferred in order to have a better fit for the near source readings. The arrival times of Pg and Sg are estimated with P and S velocities of 5.3 and 3.3 km/s for the top 12 km and 5.6 and 3.45 km/s for 12 - 16 km depth. The Pn and Sn arrival times matched with an upper-mantle P and S velocity of 5.9 km/s and 3.5 km/s, for a crustal thickness of 35 km.

Pg and Sg phases are also useful in focal depth determination. The HD method can estimate focal depths if enough data are available at close epicentral distances. In this study we initially determined a cluster depth that minimizes the trade-off between the available arrival times and the predicted traveltimes. This cluster depth is kept fixed for all the events in the cluster until the events in the cluster are stable and arrival data fit well with the theoretical travel times. Then, a free depth solution is performed for the events that have sufficient Pg and Sg data. The free depth solution determines the depths using direct phase arrivals for all the events in the cluster. However, our data sets include old earthquakes from 1970s and availability of near source data varies greatly through time. Therefore, focal depth determination for some events is done manually, using only near-source readings. This analysis revealed hypocentroid depths of 9-22 km (Fig.1) with an error of 3km.

CONCLUSIONS

Body-waveform and InSAR modeling of the 19 May 2011 Simav earthquake suggests a normal faulting mechanism with a strike of 289°, a northward dip of 54° and a centroid depth of 8 km (Fig. 2). Our preferred fault model is consistent with our calibrated earthquake locations for the Mw 5.9 main shock and its aftershocks (less than <0.5 km error in location), since they are situated on the northern side of the Simav valley.

Our calibrated new location for the Mw~7.2 Gediz earthquake is situated ~14 km southwest of its previous location (ISC) and is now more consistent with the mapped L-shaped surface rupture (Ambraseys and Tchalenko, 1972) and with Eyidogan and Jackson (1985)'s suggestion that the main shock nucleated on the NNW-SSE portion of the fault. Aftershock epicenters are concentrated on the E-W branch of the surface rupture (Fig.1) and but continue to the east, where they may delineate a previously-unrecognized active structure north of the Muratdag range.

The Demirci earthquakes, on the other hand, occurred on the western end of the Simav graben and our relocations hint that the main shock and the large aftershocks ruptured the south-dipping faults on the

northern side of the Simav graben, rather than the more clearly-expressed N-dipping fault on the south basin margin. This analysis is in good agreement with Eyidogan and Jackson (1985)'s observation for the main shock.

REFERENCES

Aktug B, Nocquet JM, Cingoz A, Parsons B, Erkan Y, England P, Lenk O, Gurdal MA, Kılıcoglu, A, Akdeniz H and Tekgul A (2009) Deformation of western Turkey from a combination of permanent and campaign GPS data: Limits to block-like behavior, *J. Geophys. Res.*, 114, B10,404, doi:10.1029/2008JB006000

Ambraseys N and Tchalenko JS (1972) Seismotectonic aspect of the Gediz, Turkey, earthquake of March 1972: *Geophysical Journal of the Royal Astronomical Society*, v. 30, p. 229–252

Bergman E and Solomon SC (1990) Earthquake swarms on the Mid-Atlantic Ridge - Products of magmatism or extensional tectonics? *Journal of Geophysical Research*, v. 95, p.4943

Bondar I, Myers SC, Engdahl ER and Bergman E (2004) Epicentre accuracy based on seismic network criteria, *Geophys. J. Int.*, 156, 483 - 496, doi:10.1111/j.1365-246X.2004.02070.x

Braunmiller J and Nabelek J (1996) Geometry of continental normal faults: Seismological constraints, J. Geophys. Res., 101, 3045 - 3052, doi:10.1029/95JB02882

Eyidoğan H and Jackson J (1985) A seismological study of normal faulting in the Demirci, Alaşehir and Gediz earthquakes of 1969–70 in western Turkey: implications for the nature and geometry of deformation in the continental crust. *Geophysical Journal International*, 81(3), 569-607

Gorgun E (2014) Source characteristics and Coulomb stress change of the 19 May 2011 Mw 6.0 Simav Kutahya earthquake, Turkey, *Journal of Asian Earth Sciences*, 87 (0), 79-88, doi: 10.1016/j.jseaes.2014.02.016

Gurboga S (2013) 28 March 1970 Gediz earthquake fault, western Turkey: palaeoseismology and tectonic significance, *International Geology Review*, 55 (10), 1191–1201, doi: 10.1080/00206814.2013.771420

Jordan TH and Sverdrup KA (1981) Teleseismic location techniques and their application to earthquake clusters in the South-Central Pacific: *Bulletin of the Seismological Society of America*, v. 71, no. 4, p. 1105–1130

McKenzie D (1978) Active tectonics of the Alpine-Himalayan belt: the Aegean Sea and surrounding regions, *Geophys. J. R.* Astron. Soc., 55 (1), 217-254, doi:10.1111/j.1365- 246X.1978.tb04759.x

Okada Y (1985) Surface deformation due to shear and tensile faults in a half-space, *Bull. Seismol. Soc. Am.*, 75, 1135{1154

Seyitoglu G (1997) Late Cenozoic tectono-sedimentary development of Selendi and Usak-Gure basins: a contribution to the discussion on the development of east-west and north- trending basins in western Turkey, *Geol. Mag.*, 134, 163-175

Tasdemiroglu M (1971) The 1970 Gediz earthquake in Western Anatolia, Turkey, *Bull. Seismol. Soc. Am.*, 61, 1507-1527

Vanacore E, Taymaz T and Saygın EE (2013) Moho structure of the Anatolian Plate from receiver function analysis, *Geophys. J. Int.*, 193 (1), 329–337, doi:10.1093/gji/ggs107

Walker RT, Bergman EA, Szeliga W and Fielding EJ (2011) Insights into the 1968-1997 Dasht-e-Bayaz and Zirkuh earthquake sequences, eastern Iran, from calibrated relocations, InSAR and high-resolution satellite imagery: *Geophys. J. Int.*, p. no 187, 1577–1603, doi: 10.1111/j.1365-246.2011.05213

Yolsal-Cevikbilen S, Taymaz T and Helvaci C (2014) Earthquake mechanisms in the Gulfs of Gokova, Sigaci, Kusadasi, and the Simav Region (western Turkey): Neotectonics, seismotectonics and geodynamic implications, *Tectonophys.*, 635, 100-124, doi: 10.1016/j.tecto.2014.05.001

Zulfikar C, Kamer Y and Vuran E (2011) May 19, 2011 Kutahya-Simav Earthquake, Tech. rep., Bogazici University, Kandilli Observatory and Earthquake Reserach Institute, Bebek-Istanbul